IET Biometrics

Research Article

IET Journals
The Institution of Engineering and Technology

ISSN 2047-4938
Received on 10th July 2015
Revised on 6th November 2015
Accepted on 11th January 2016
doi: 10.1049/iet-bmt.2015.0048
www.ietdl.org

Comparison of quasi-spherical surfaces – application to corneal biometry

Arnaud Polette[1,2] ✉, *Jean-Luc Mari*[1], *Isabelle Brunette*[3], *Jean Meunier*[2,4]

[1]*Aix-Marseille Université, CNRS, LSIS UMR 7296, Marseille, France*
[2]*Department of Computer Science and Operations Research, University of Montreal, Montréal, Canada*
[3]*Maisonneuve-Rosemont Hospital, Department of Ophthalmology, University of Montreal, Canada*
[4]*Biomedical Engineering Institute, University of Montreal, QC, Canada*
✉ *E-mail: arnaud.polette@univ-amu.fr*

Abstract: In this study, the authors present two new techniques with their own particular advantages dedicated to the authentication of a person based on the three-dimensional geometry of the cornea. A device known as corneal topographer is used for capturing the shape of each cornea. Until now only a few studies on corneal biometry have been conducted and they were limited only to the anterior surface. In this study, since the whole cornea is a tissue layered by two (anterior and posterior) surfaces, the authors propose to use both surfaces to characterise the corneal shape. The first proposed method consists of comparing coefficients from a spherical harmonics decomposition, and this allows to do a fast comparison that can be used to perform many-to-one comparisons. The second approach is based on the minimal residual volume between two corneas after a registration step, this geometry-based method is more accurate but slower, and is thus used to perform one-to-one comparisons. A cascade fusion scheme is also proposed to benefit from the advantages of both methods. The authors' study demonstrates that corneal shape could be used for biometry. The two proposed methods have been tested and validated on a dataset of 257 corneas.

1 Introduction

Nowadays, biometric recognition is commonly used to identify a person using characteristic features of the human body. Several parts are used: fingerprints, footprints, iris, venous networks, facial shape, and so on. In this study, we propose to use another part of the human body: the cornea. Cornea is the outer part of the eye, it can be measured without contact with a corneal topographer (frequently used by ophthalmologists). Several studies aimed at comparing corneal surfaces, mainly for medical purposes: comparison of groups of different surgeries [1], of different age ranges [2], of different disease stages [3], of subjects for a stability study of corneal topography in the post-blink interval [4], for determining differences with an average model for a repeatability study [5], for construction of medical atlases [6] and so on. The two main academic investigations that focus on the comparison of corneal surfaces for a biometric application are [7] using a Zernike polynomial decomposition [8] and our preliminary work [9] with spherical harmonics decomposition. However, both were limited to the anterior surface only. Also, two patents propose the general idea of corneal biometry [10, 11], one of them suggesting to use the fact that the posterior corneal surface is inside the eye, which makes it very difficult to falsify.

Our approach aims at combining both anterior and posterior corneal surfaces to obtain a better recognition rate with a good level of security. An application of this approach in the future could be the use of a multiple modality eye recognition system including the cornea (geometric information) combined with the retina (vascular tree structure information) and the iris (texture information). We can easily imagine a multiple modality measuring system that could capture all at the same time.

In this paper, we present two new methods (and a conceivable fusion scheme) to compare corneas, using both anterior and posterior surfaces to improve separability. The first approach is based on a spherical harmonics decomposition and the second one is based on a registration technique aiming at determining the minimal residual volume between corneas to be compared, these methods give *equal error rate* (EER) values of 2.7 and 1.2%, respectively.

The first one provides a fast comparison to perform a biometric identification by storing only few discriminant coefficients (i.e. comparing one cornea to a large database). The second one is geometry based, and need to store and to compute the whole geometry to consider thin details of the corneal shape more accurately. It can be suitable for biometric verification purposes which only need a one-to-one comparison (to verify if the person is who he/she claims to be). These two methods could be used separately for two different purposes, or jointly in a cascade fusion architecture to use the accuracy of the second method to check the output of the first method.

The paper is organised as follows. First, a review of the basic concepts about the cornea is presented, and then Zernike and spherical harmonics decomposition are detailed, followed by a description of our two methods. Then both methods are tested and compared with the existing ones with real data. A receiver operation characteristic (ROC) curve analysis is then presented. It shows better performance with the two proposed methods. The particular advantages of each method are discussed in the final section.

2 Basic notions and previous work

2.1 Corneal basic concepts

The cornea is the transparent outer front part of the eye. It covers nearly a fifth of the eye's surface, with an average diameter of 11 mm. It is the main lens of the eye, responsible for two-thirds of the dioptric power (the remaining third is the eye crystalline lens), with a refractive index of 1.377. The cornea is slightly thicker at its periphery: ~0.5 mm at the centre and 0.6 mm at the periphery. The curvature radius of the anterior surface varies between 7 and 9 mm and is ~6.5 mm for the posterior surface. A cross-sectional schematic view of an eye is presented in Fig. 1 showing both anterior and posterior surfaces.

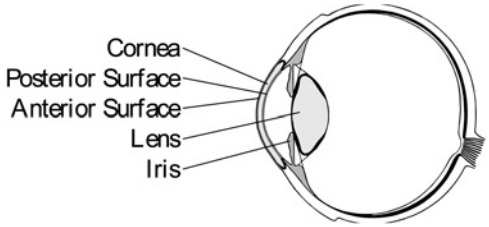

Fig. 1 *Sectional view of the eyeball*

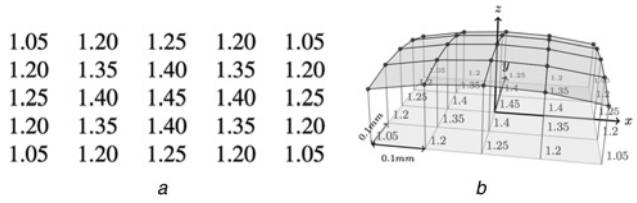

Fig. 2 *Surface mesh construction step from Orbscan II raw data*

a Orbscan II raw data
b Mesh built from elevations

Different corneal topographers exist for capturing the three-dimensional (3D) shape of the cornea such as the PENTACAM® (Oculus) and the ORBSCAN II® (Bausch & Lomb). The ORBSCAN II® was used in this study to acquire elevation maps of both the anterior and posterior surfaces, with an error margin of 1 µm. The data were saved as a uniformly spaced 101×101 grid of elevations, spaced by 0.1 mm along the *X*- and *Y*-axes. Fig. 2*a* shows an example of raw ORBSCAN II® data. Fig. 2*b* presents the method for constructing the mesh from the elevations. The points are elevated and linked by edges to their neighbours to build faces. Each measured cornea consists of two mesh surfaces (anterior and posterior) bounding the corneal volume.

As the cornea is almost spherical, a smart and efficient way to visualise the global appearance of a corneal surface is to use a spherical reference, which makes it possible to study the differences from a sphere. First, the centre and radius of the best fit sphere (BFS) are calculated by a least square minimisation of the sum of distances between the sphere and the corneal surface [12]. Then, the difference between the corneal surface and the BFS surface is estimated at each point. Finally, each difference is associated with a colour, using a standard colourset (commonly used by the clinician), with *warm* colours for positive differences (points outside the BFS) and *cold* colours for negative differences (points inside the BFS). The colours are then projected on a plane perpendicular to the *Z*-axis to get a colour map useful for diagnostic interpretation.

Fig. 3 shows the construction steps of the colour map (displayed in greyscale in the figure). Ophthalmologists commonly use these maps for diagnosis purposes. Usually the BFS radius for corneal surfaces is around 7 ± 2 mm. The colour range of the difference map from a sphere shows that the corneal surface is very close to a sphere.

2.2 Data acquisition procedure

The acquisition system used for this study is the ORBSCAN II® (Bausch & Lomb), but any topographer that provides 3D representations of the cornea can be used. Usually, in the medical context, the corneal topography is performed with the subject seated with his eye in front of the capture system for a few seconds (Fig. 4). The capture is not invasive and contactless. The

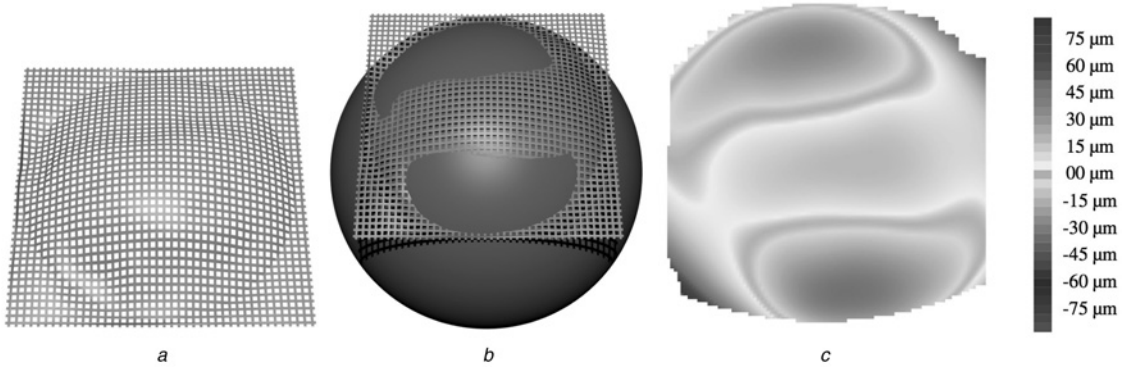

Fig. 3 *Colour map building steps, this example shows a right anterior corneal surface*

a Height map
b BFS height map
c Colour map

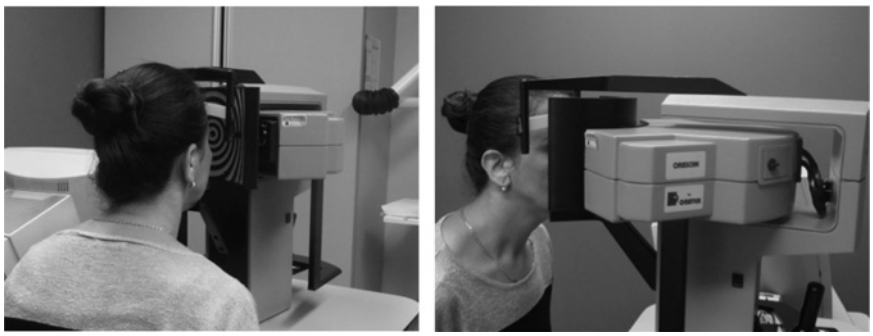

Fig. 4 *Data acquisition*

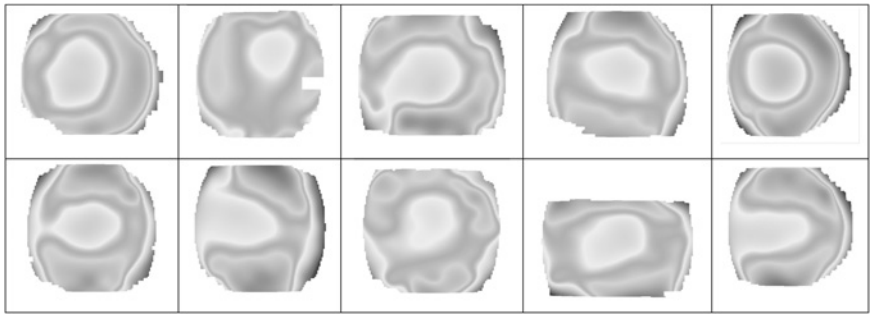

Fig. 5 *Ten acquisitions of different subjects*

Table 1 Zernike coefficients and indexes

	−2	−1	0	1	2	*m*
0			$C_0^0(1)$			
1		$C_1^{-1}(2)$		$C_1^1(3)$		
2	$C_2^{-2}(4)$		$C_2^0(5)$		$C_2^2(6)$	
n						

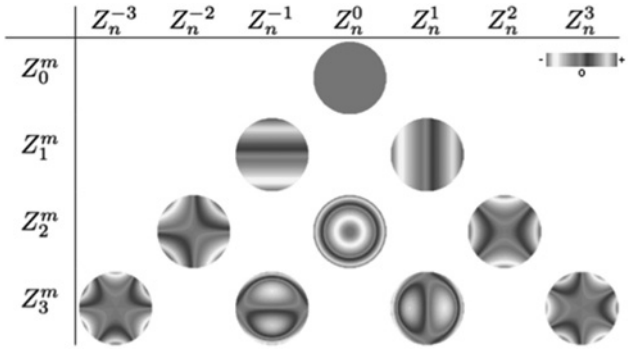

Fig. 6 *Ten first Zernike polynomials*

Table 2 Spherical harmonics coefficients and indexes

	$m=-2$	$m=-1$	$m=0$	$m=1$	$m=2$
$l=0$			$C_0^0(1)$		
$l=1$		$C_1^{-1}(2)$	$C_1^0(3)$	$C_1^1(4)$	
$l=2$	$C_2^{-2}(5)$	$C_2^{-1}(6)$	$C_2^0(6)$	$C_2^1(7)$	$C_2^2(8)$
…	…	…	…	…	…

corneal acquisition procedure is similar to the iris acquisition procedure; therefore we can consider that the cornea has the same user acceptability as the iris. Being physically close to the iris, we can also assume that the universality of this modality is also close to the iris. For now a corneal topographer is relatively expensive (around $50 K) but this price tag could diminish with its wider use for biometrics and could be in the future designed specifically for biometric purposes.

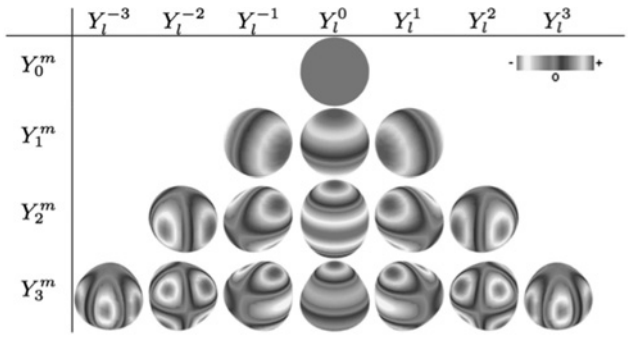

Fig. 7 *Sixteen first spherical harmonics*

2.3 Previous work on corneal biometry: comparison of Zernike polynomials coefficients

Fig. 5 shows ten acquisitions of different subjects. They illustrate the variability for different subjects. This visually demonstrates the potential of corneal shape for biometry. Consequently, in his thesis, Lewis [7] uses a Zernike polynomial decomposition [8] on the anterior surface as shape descriptors, in order to compare two anterior corneal surfaces for biometric purposes. We now describe this polynomial decomposition in more details.

Any elevation surface $f(r, \theta)$ can be decomposed in a weighted sum of Zernike polynomials Z_n^m over the unit circle, where θ is the azimuthal angle, r the radial distance, n and m integers ($n \geq m$) are as follows

$$f(r, \theta) = \sum_{n=0}^{+\infty} \sum_{m=-n}^{n} C_n^m \cdot Z_n^m(r, \theta) \tag{1}$$

n is called the degree, and m is the order, with $n - m$ even.

Zernike polynomials are defined as follows:

$$Z_n^m(r, \theta) = R_n^m(r) \cos(m\theta) \quad \text{(even)} \tag{2}$$

$$Z_n^{-m}(r, \theta) = R_n^m(r) \sin(m\theta) \quad \text{(odd)} \tag{3}$$

where

$$R_n^m(r) = \sum_{s=0}^{(n-m/2)} \frac{(-1)^s (n-s)!}{(s)!\big((n+m/2)-s\big)!\big((n-m/2)-s\big)!} r^{n-2s} \tag{4}$$

Each coefficient is associated to an index (see Table 1).

This formalism makes possible the representation of a surface with only an indexed array of coefficients. Fig. 6 shows the first ten Zernike polynomials from Z_0^0 to Z_3^3 as elevations over the unit circle.

A surface can be decomposed into an array of coefficients using a Zernike polynomials least-square fit to this surface [8].

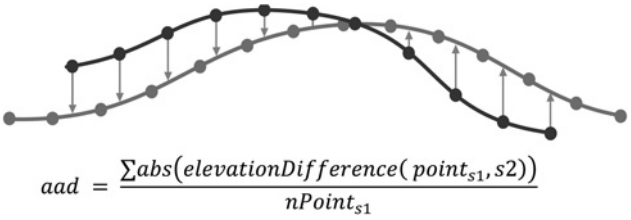

Fig. 8 *aad with surface 1 in black and surface 2 in grey*

IET Biom., 2016, Vol. 5, Iss. 3, pp. 212–219

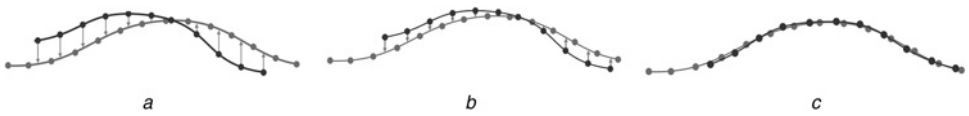

Fig. 9 *Registration of two surfaces*

a Initialisation
b aad minimisation
c aad is minimal, the registration is complete

The approach proposed by Lewis [7] deals with the comparison of arrays (C_0^0 to $C_7^7 = 36$ values) of Zernike coefficients after a decomposition to determine if compared surfaces are from the same person. Each coefficient is compared one-by-one and then differences are summed

$$\text{dist}(s_1, s_2) = \sum_x \left(|s_1 C_x - s_2 C_x| \right) \tag{5}$$

s_1C_x and s_2C_x being the coefficient arrays of compared surfaces s_1 and s_2. The author proposes to delete C_0^0, C_1^{-1} and C_1^1 from the sum, because he observed that the variability within different acquisitions from a same subject was too high. Those coefficients (C_0^0, C_1^{-1} and C_1^1) correspond, respectively, to the global mean elevation (Piston), the *X*-lateral position and the *Y*-lateral position. They are not dependant on the corneal shape, but on the position of the cornea during the acquisition.

However, according to [13], the use of a spherical harmonics decomposition gives a better fit to a corneal surface than Zernike polynomials for the same number of coefficients. For this reason, we tested spherical harmonics (see next section) for corneal biometry in another study [9] with promising results. However both methodologies use only one (anterior) of the two corneal surfaces, this means the whole corneal shape is not considered in totality.

3 Description of the methods

In this section, we present two new techniques with their own particular advantages dedicated to the authentication of a person

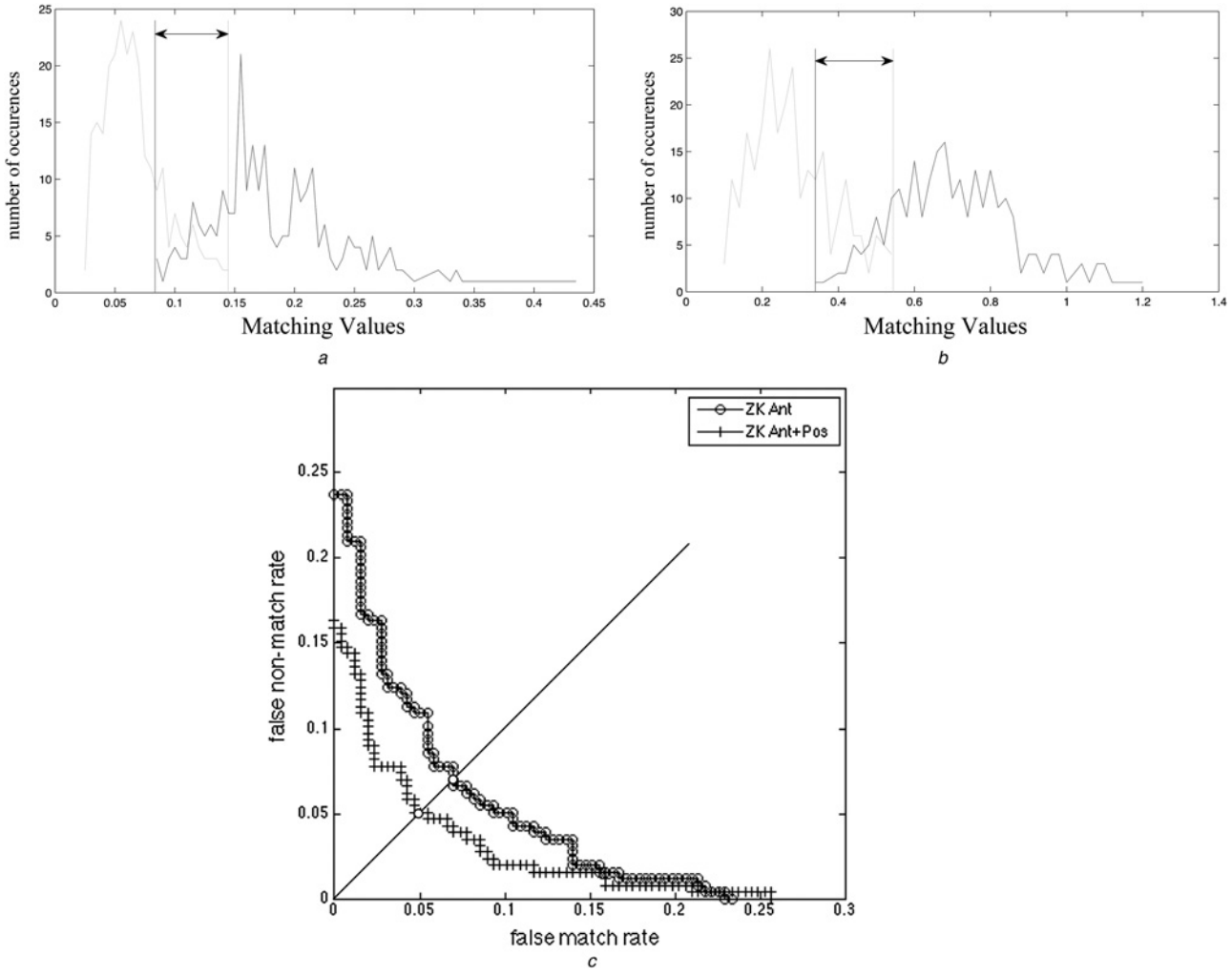

Fig. 10 *Results using a Zernike coefficients comparison*

a Using the anterior surface only
b Using both anterior and posterior surfaces
c ROC curve comparison of the Zernike method using one (circle) and two (plus) surfaces, the nearer to the origin is the curve, the better

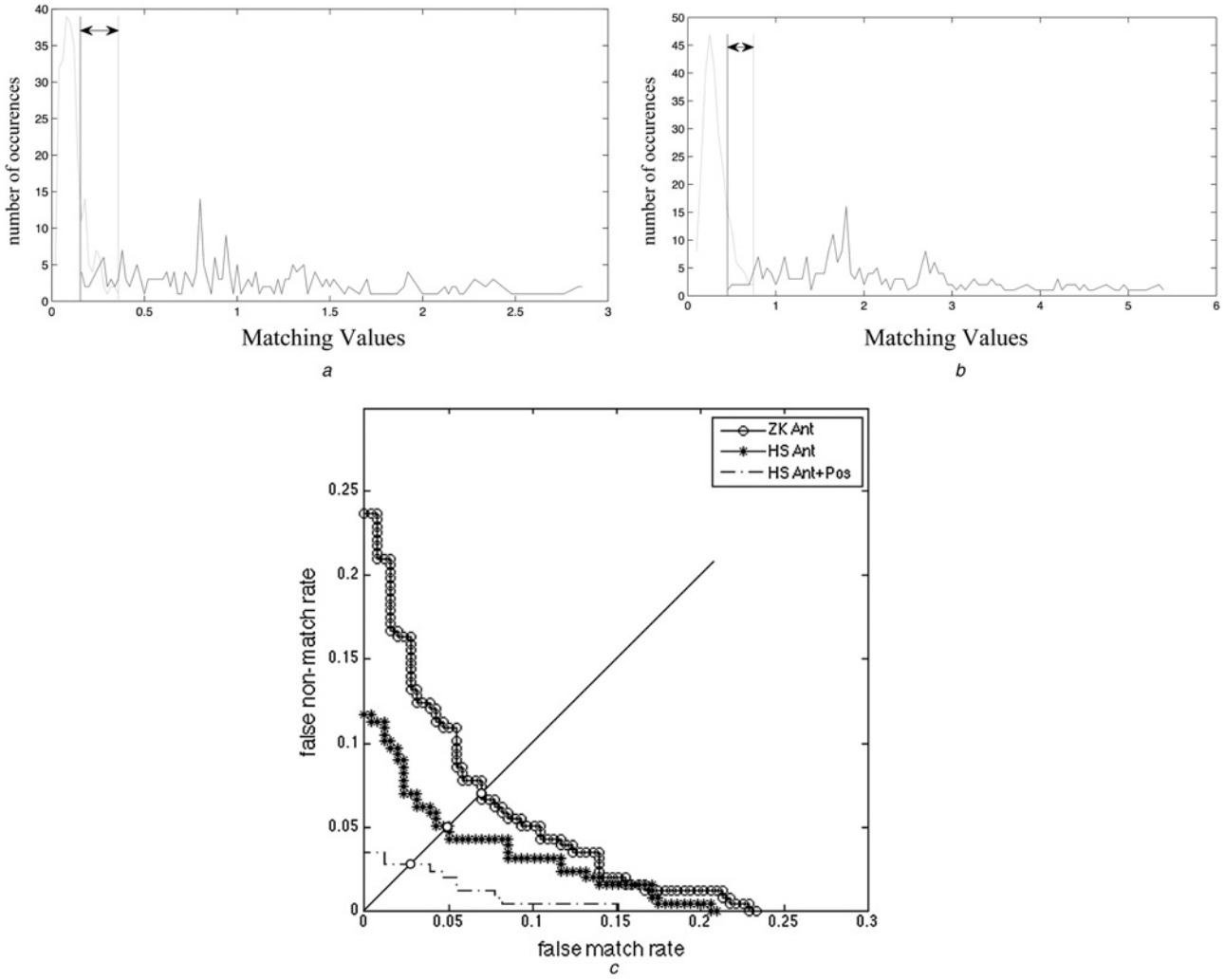

Fig. 11 *Results using a spherical harmonics coefficients comparison*

a Using the anterior surface only
b Using both anterior and posterior surfaces
c ROC curve comparison of the Zernike method (circle), and the spherical harmonics method using one (asterisk) and two (dot-dash) surfaces, the nearer to the origin is the curve, the better

based on the 3D shape of cornea. The whole cornea is considered by using the two (anterior and posterior) surfaces.

3.1 Method 1: Corneal biometry using spherical harmonics coefficients comparison

Spherical harmonics are a suitable mathematical model for quasi-spherical shapes. Considering our preliminary good results reported in [9], this first method uses spherical harmonics coefficients as shape descriptor to compare surfaces instead of using Zernike coefficients. In addition, in this new approach, both surfaces are represented instead of the anterior surface only.

3.1.1 Spherical harmonics decomposition: Any surface $f(\theta, \varphi)$ can be decomposed in a sum of $2l+1$ spherical harmonics $Y_l^m(\theta, \varphi)$, with $-l \leq m \leq l$, weighted by a coefficient C_l^m, where l and m are integers, as follows

$$f(\theta, \varphi) = \sum_{l=0}^{+\infty} \sum_{m=-l}^{+l} C_l^m \cdot Y_l^m(\theta, \varphi) \tag{6}$$

$Y_l^m(\theta, \varphi)$ is defined as follows:

$$Y_l^m(\theta, \varphi) = \sqrt{\frac{2(l-m)!}{(l+m)!}} \cdot P_l^m(\cos\theta) \cdot \cos(m\varphi) \tag{7}$$

With the Legendre functions

$$P_l^m(x) = \frac{(-1)^m}{2^l l!}\left(1-x^2\right)^{(m/2)} \frac{\mathrm{d}^{m+l}}{\mathrm{d}x^{m+l}}\left(x^2-1\right)^l \tag{8}$$

Each coefficient is associated to an index (see Table 2).

Thus, it is possible to represent a surface with only an array of coefficients. Fig. 7 shows the 16 first spherical harmonics from Y_0^0 to Y_3^3 relatively to a unit sphere.

3.1.2 Spherical harmonics coefficients comparison: To decompose a corneal surface into spherical harmonics, the surface is first centred on a spherical reference, by locating the BFS on the coordinate system origin. By doing that, all the spherical information is contained in the first coefficient C_0^0, all the other coefficients represent the relative deformations to a sphere.

To compare fairly our method to the Zernike approach, surfaces are decomposed in the same number of coefficients, from C_0^0 to C_5^5 (36 coefficients), by least-square fitting to the surface.

Our distance computation is close to the previous one (for the Zernike approach), using spherical harmonics coefficients, but the difference is computed with all coefficients

$$\mathrm{dist}(s_1, s_2) = \sum_x \left(\left|s_1 C_x - s_2 C_x\right|\right) \tag{9}$$

IET Biom., 2016, Vol. 5, Iss. 3, pp. 212–219

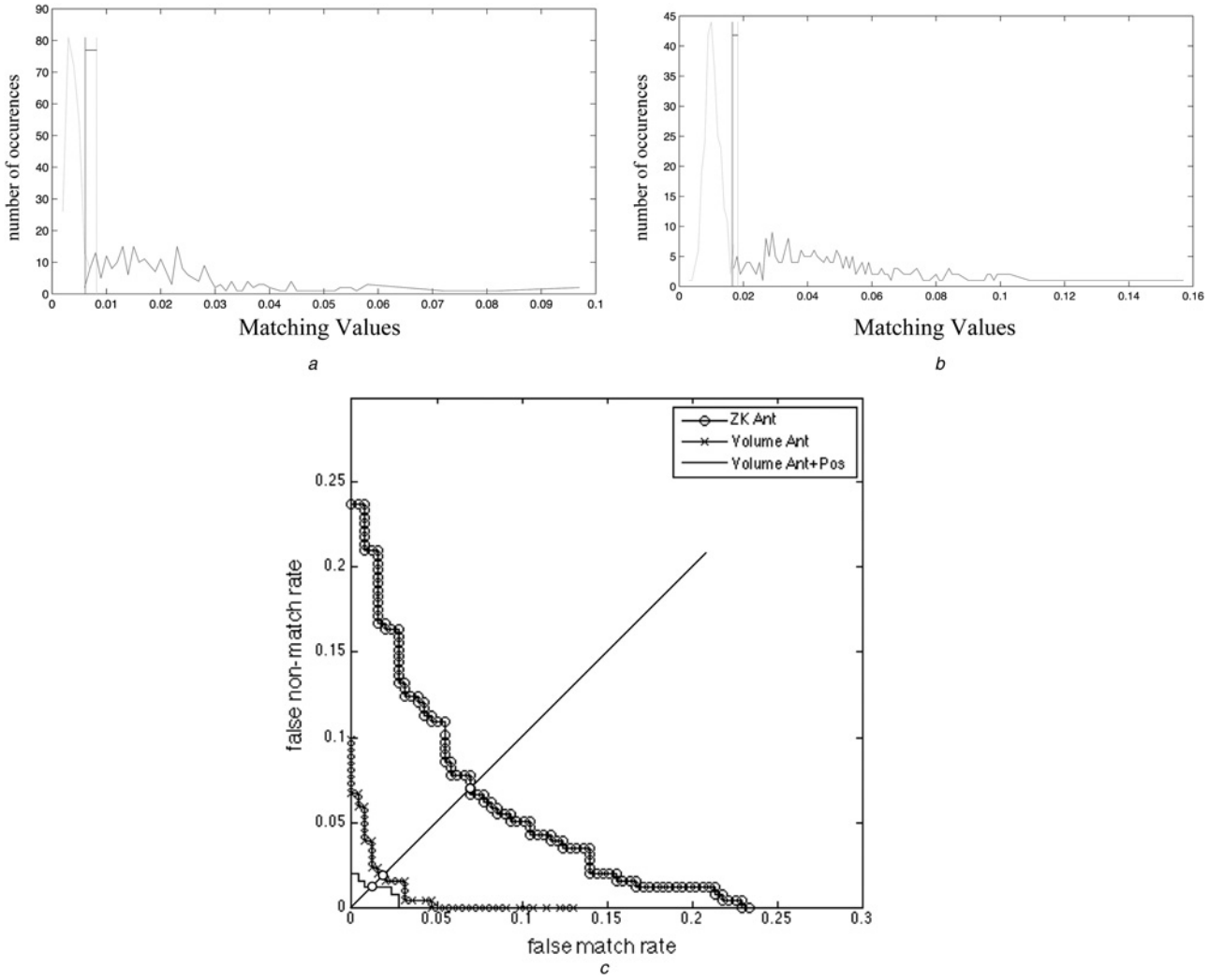

Fig. 12 *Matching values using inter-surface residual volume comparison*

a Using the anterior surface only
b Using both anterior and posterior surfaces
c ROC curve comparison of the Zernike method (circle), and inter-surface residual volume comparison method using one (cross) and two (solid) surfaces, the nearer to the origin is the curve, the better

This method can be used with two (anterior and posterior) surfaces by summing the distance of the two surfaces to obtain a distance value for the whole cornea (see [9]).

3.2 Method 2: Corneal biometry using inter-surface residual volume

Here, the aim is to compute a representative value of the real geometrical difference between a pair of surfaces (pair of anterior and pair of posterior surfaces for cornea) to be compared. Evidently, the naive direct subtraction of elevation maps does not work because the corneas are not necessarily properly aligned. The key idea is to perform a registration of a surface to another by minimising the overlap in-between volume between the two surfaces. The residual volume is then a representative value of the difference between two surfaces: the closer to 0 this value is, the more similar the surfaces. Thus the method is based on the minimisation of this residual volume computed as the *average absolute elevation difference* from a surface to another on overlapping parts of surfaces after registration (see [9]).

A point to face elevation difference (arrows in Fig. 8) is determined by a bilinear interpolation of the elevation on a face from the coordinates of a point of the other. This difference is noted elevation Difference(p, s) in the following equation of the *average absolute difference* (*aad*), with s_1 and s_2 two surfaces, point_{s_1} a point from s_1 and n_{s_1} the point number in s_1 in Fig. 8.

The *aad* is then minimised with a non-linear optimisation algorithm (Fig. 9) based on the Nelder–Mead method [14] (available in GSL, the GNU *Scientific Library* [15]).

After the registration step (Fig. 9*c*), the residual *aad* is representative of the minimal existing average volume between two surfaces, which can be used as a similarity descriptor. This method can also be used with two (anterior and posterior) surfaces by summing the minimal existing average volume of the two (anterior to anterior and posterior to posterior) surfaces to obtain a distance value for the whole cornea.

4 Results and discussion

To quantify the error margin of each method, a set of matching-comparisons (comparisons between two corneas from the same eye) and a set of non-matching-comparisons (comparisons between two corneas from different eyes) are computed to observe the variability of each matching case, and how the error margins (identified by the overlapping range between the two sets of values) are large.

4.1 Dataset

Our dataset contains 2 different acquisitions of 257 corneas (total of 514 corneal topographies), with 120 from right eyes and 137 from

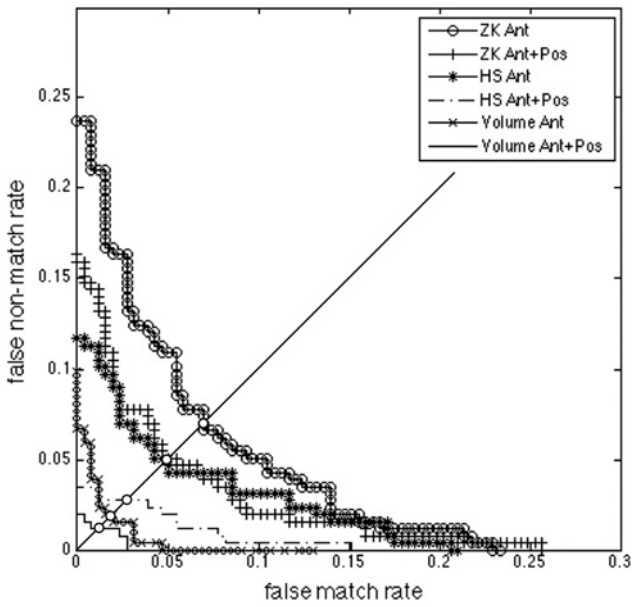

Fig. 13 *All results grouped on a ROC curve*

left eyes. This allows to compute up to 257 matching-comparisons. Non-matching-comparisons are computed with randomly chosen pairs of right or left corneas.

4.2 Results with Zernike coefficients

To compare our methods to the existing ones, matching values have been computed first with Zernike coefficients (Section 2.2). Results are presented in Figs. 10*a* and *b*, with 257 matching-comparisons in light grey, and 257 non-matching-comparisons in dark grey. The overlapping range between matching-comparisons values and non-matching-comparisons values (emphasised with an arrow in Figs. 10*a* and *b*) is the error margin. A potential discrimination threshold can be set in this range. The threshold position between these two values determines the false-match-rate (false-positive-rate) and the false non-match rate (false-negative-rate) and allows the construction of the ROC curve presented in Fig. 10*c*. The closer the curve is to the origin (lower left corner), the better the method is to predict correct matching of corneas.

We can observe that the use of a second (posterior) surface provides a more efficient discrimination of the two groups of measures than the anterior surface alone used in the work of Lewis [7]. This allows achieving an EER of 5.1% (F1-Score = 0.95 and MCC = 0.9) with two surfaces while only one gives 7% (F1-Score = 0.93 and MCC = 0.86).

4.3 Results with spherical harmonics coefficients

The same set of measures was generated using spherical harmonics to compute matching values in Figs. 11*a* and *b* and the corresponding ROC curve in Fig. 11*c*.

Using only one surface with the same number of coefficients allows to discriminate more efficiently the two groups of measures using the spherical harmonics decomposition with an EER of 5.1% (F1-Score = 0.95 and MCC = 0.9, asterisk curve Fig. 11*c*) than the Zernike decomposition (circle curve, Fig. 11*c*), and the EER decreases even more while using two surfaces with a value of 2.7% (F1-Score = 0.97 and MCC = 0.94, dot-dash curve Fig. 11*c*).

4.4 Results using inter-surface residual volume

The results of our second method are presented in Figs. 12*a*–*c*, using the same dataset.

As for Zernike and spherical harmonics, the error decreases from an EER of 2% (F1-Score = 0.98 and MCC = 0.96) to 1.2% (F1-Score = 0.99 and MCC = 0.98) when adding the second surface (Fig. 12c solid ROC curve).

5 Discussion

All ROC results have been reported on a common graph in Fig. 13 showing the performance of all approaches. The method proposed by Lewis [7] with a Zernike polynomial decomposition is the least efficient (circle curve) with an EER value of 7%. Our previous work [9] with spherical harmonics decomposition of the anterior surface gives better results (asterisk curve) with an EER value of 5.1%, the addition of the posterior surface to this method reduced the EER to 2.7%. Finally, the residual inter-surface volume approach is best with EER values of 2 and 1.2% using one and both surfaces, respectively. As expected, the use of the second (posterior) surface is helpful for all approaches, i.e. Zernike polynomials, spherical harmonics or residual volume. The best overall performance using both surfaces is obtained with the inter-surface residual volume method (cross curve) with an EER value of 1.2% followed closely by spherical harmonics (dot-dash curve) with an EER value of 2.7%. Notice that the residual volume method is better for all thresholds of the ROC curves. In addition, in an identification context the inter-surface residual volume method gives a rank-one value of 97.2%.

Although the spherical harmonics method is the second best method (based on EER), it is the best method based on coefficient comparisons. This fact is important because a method based on coefficients allows the storage of a small number of values (only 36 values here) for each surface, and therefore searching for a cornea is much faster. For example, biometric identification (i.e. comparing one cornea to a large database) is possible with this method and would take only a few seconds for a dataset composed of thousands corneas.

The inter-surface residual volume method gives the best matching rate but needs to store the entire corneal geometry (in this study: two 101×101 matrices of elevation values), and would take a few seconds for only one comparison. This method can be suitable for biometric verification purposes, which only needs a one-to-one comparison to verify if the person is who he/she claims to be.

Therefore, both methods (spherical harmonics and residual volume) have their own specific advantages and application fields for biometry. Moreover, they could be combined in a serial (or cascade) fusion architecture (e.g. [16]) to take advantage of the accuracy of the residual volume method to check the output of the much faster spherical harmonics method (see Fig. 14). In this serial scheme, biometric identification is done with the fastest method first (i.e. spherical harmonics) to prune the database. If a computed distance is lower than a predefined lower threshold, the subject is immediately identified (true match), without further processing. This threshold can be chosen to get the false match rate = 0 to guarantee that no false positive occurs. Conversely, if the distance is more than another predefined upper threshold, the current enrolled individual of the database is immediately rejected (true non-match). This threshold can be set to get the false non-match

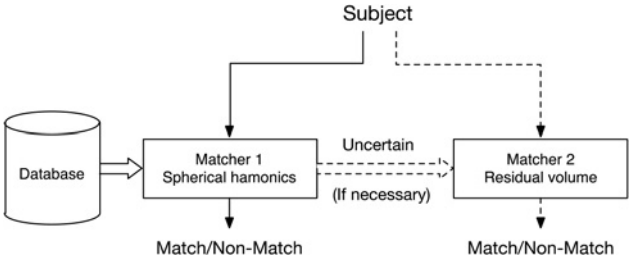

Fig. 14 *Cascade fusion architecture*

IET Biom., 2016, Vol. 5, Iss. 3, pp. 212–219

rate = 0 to guarantee that no false negative occurs. Computed distances between these two thresholds are uncertain and require using a second matcher (residual volume) to identify the subject. This kind of fusion strategy will greatly reduce the computation time required by using the residual volume method alone by eliminating 'easy' cases with the faster spherical harmonics method. In our study, with spherical harmonics of both surfaces, only 9.3% (overlapping region in Fig. 11*b*) of the database would need further processing with the more accurate but slower residual volume method.

In comparison with some other modalities, corneal biometry is certainly promising. For instance, the 3D ear shape can achieve an EER value of 1.2% [17], which is similar to our best results. Other biometric traits such as gait are typically inferior with the EER value around 5% or higher [18]. Other modalities such as fingerprints are better (e.g. EER ranging from 0.2 to 0.4% [19]) but one should take into account that our study is only a first step in this new domain and that corneal measures could be combined with others (iris, retina) within the same apparatus in the future.

6 Conclusion

In this paper, two new methods are presented to compare pairs of quasi-spherical surfaces in the context of corneal biometry. The first one uses a spherical harmonics coefficient comparison and the second one is based on a direct mesh comparison after a prior registration. Both proposed methods gave better results than classical Zernike polynomials decomposition. In addition, they can easily be combined in a serial fusion scheme. This study also shows clearly that corneal shape is suitable as a biometric feature.

Both methods could be improved in the future. The coefficient-based method uses a basic comparison of the coefficients considering them one-by-one. Although this approach was efficient, it can be enhanced by determining which coefficient contributes the most to the surface discrimination (feature selection) or by extracting new more powerful features from them (feature extraction e.g. with LDA: linear discriminant analysis). As for the residual volume comparison it could also be improved by adding other features such as the corneal thickness as a part of the discriminating features to represent in a better way the whole corneal volume (instead of its two surfaces only). In addition, it would be interesting to conduct a long-term repeatability study since the cornea might slowly evolve with age, to determinate how often a corneal database would need to be updated.

7 Acknowledgment

The authors thank the Quebec Vision Health Research Network for its support.

8 References

1 Hayashi, K., Nakao, F., Hayashi, F.: 'Corneal topographic analysis of superolateral incision cataract surgery', *J. Cataract Refract. Surg.*, 1994, **20**, (4), pp. 392–399
2 Hayashi, K., Hayashi, H., Hayashi, F.: 'Topographic analysis of the changes in corneal shape due to aging', *Cornea*, 1995, **14**, (5), pp. 527–532
3 Brunette, I., Sherknies, D., Terry, M., *et al.*: '3-D, characterization of the corneal shape in Fuchs dystrophy and pseudophakic keratopathy', *Invest. Ophthalmol. Vis. Sci.*, 2011, **52**, (1), pp. 206–214
4 Buehren, T., Collins, M.J., Iskander, D.R., *et al.*: 'The stability of corneal topography in the post-blink interval', *Cornea*, 2001, **20**, (8), pp. 826–833
5 Fam, H.-B., Lim, K.-L., Reinstein, D.Z.: 'Orbscan global pachymetry: analysis of repeated measures', *Optom. Vis. Sci.*, 2005, **82**, (12), pp. 1047–1053
6 Laliberté, J.F., Meunier, J., Chagnon, M., *et al.*: 'Construction of a 3-D atlas of corneal shape', *Invest. Ophthalmol. Vis. Sci.*, 2007, **48**, (3), pp. 1072–1078
7 Lewis, N.D.: 'Corneal topography measurements for biometric applications'. PhD dissertation, The University of Arizona, 2011
8 Iskander, D.R., Collins, M.J., Davis, B.: 'Optimal modeling of corneal surfaces with Zernike polynomials', *IEEE Trans. Biomed. Eng.*, 2001, **48**, (1), pp. 87–95
9 Polette, A., Mari, J.-L., Brunette, I., *et al.*: 'Comparison of quasi-spherical surfaces using spherical harmonics: application to corneal biometry'. Fourth Int. Conf. on Image Processing Theory, Tools and Applications (IPTA), 14–17 October 2014, pp. 308–312
10 Ramos, C.S.: 'Biometric recognition through examination of the surface map of the second ocular dioptric'. Google Patents US20110058712, 2011
11 Mason, S.: 'Corneal biometry apparatus and method'. Google Patents US20070291997, 2007
12 Gatinel, D., Malet, J., Hoang-Xuan, T., *et al.*: 'Corneal elevation topography: best fit sphere elevation distance, asphericity, toricity, and clinical implications', *Cornea*, 2011, **30**, (5), pp. 508–515
13 Iskander, D.R.: 'Modeling videokeratoscopic height data with spherical harmonics', *Optom. Vis. Sci.*, 2009, **86**, (5), pp. 542–547
14 Nelder, J., Mead, R.: 'A simplex method for function minimization', *Comput. J.*, 1965, **7**, (4), pp. 308–313
15 Gough, B.: 'GNU scientific library reference manual - third edition' (Network Theory Ltd, 2009)
16 Marcialis, G.L., Roli, F., Didaci, L.: 'Personal identity verification by serial fusion of fingerprint and face matchers', *Pattern Recognit.*, 2009, **42**, (11), pp. 2807–2817
17 Yan, P., Bowyer, K.W.: 'Biometric recognition using 3D ear shape', *IEEE Trans. Pattern Anal. Mach. Intell.*, 2007, **29**, (8), pp. 1297–1308
18 Gafurov, D., Helkala, K., Søndrol, T.: 'Biometric gait authentication using accelerometer sensor', *J. Comput.*, 2006, **1**, (7), pp. 51–59
19 Luo, H., Yu, F.-X., Pan, J.-S., *et al.*: 'A survey of vein recognition techniques', *Inf. Technol. J.*, 2010, **9**, pp. 1142–1149